Crystal Structures, Dynamic Behaviour and Electrochemical Properties of the Copper-(I) and -(II) Complexes of a New N$_2$S$_2$ Ligand†

**David A. Nation, Max R. Taylor and Kevin P. Wainwright** *
School of Physical Sciences, The Flinders University of South Australia, GPO Box 2100, Adelaide, South Australia 5001, Australia

The complexing properties of the new quadridentate N$_2$S$_2$ ligand N,N'-bis$\{$[2-(phenylmethylthio)phenyl]-methylene$\}$ethane-1,2-diamine, L, with Cu^I and Cu^{II} have been investigated. The perchlorate salt of [CuL]$^+$ occurs as orange crystals in which mirror image forms, [($\pm$)-(R^*,R^*S^*)], of the highly distorted tetrahedral cation coexist. The CuN$_2$–CuS$_2$ dihedral angle = 60.0(1)°, bond lengths and angles are Cu–S 2.285(1) and 2.258(1) Å, Cu–N 2.029(3) and 2.069(3) Å, N–Cu–N 82.7(1)°, S–Cu–S 123.56(4)°. In nitromethane solution, however, variable-temperature ^{13}C NMR spectroscopy indicates that [CuL]$^+$ exists predominantly as an equilibrium mixture of the two other diastereomers, [($\pm$)-(R^*,R^*,R^*)] and [($\pm$)-R^*,S^*,S^*)] for which the interconversion barrier corresponds to $\Delta G^\ddagger_{280}$ = 59.8 ± 0.6 kJ mol^{-1}. Exposure of an ethanolic solution of [CuL]ClO$_4$ to the atmosphere leads to slow deposition of brown crystals of [CuL(H$_2$O)][ClO$_4$]$_2$. Crystal structure determination revealed the Cu^{II} cation to be square-pyramidal with the water molecule occupying the apical position: Cu–S 2.323(6) and 2.318(5) Å; Cu–N 1.94(1) and 2.00(2) Å; Cu–O (H$_2$O) 2.29(1) Å. The crystals are achiral and racemic, arising through coexistence of the [($\pm$)-(R^*,R^*)] enantiomeric forms of the complex. Cyclic voltammetry indicates a quasi-reversible system for which $E_\frac{1}{2}$ = 0.28 V vs. saturated calomel electrode.

Since it became established that the copper binding site in blue copper proteins consists of two imidazole-N atoms from two histidine residues, a thiolato-S atom from a cysteine residue and a thioether-S atom from a methionine residue there has been intense interest in copper co-ordination chemistry involving N$_2$S$_2$ ligands. As these metalloproteins operate as electron-transfer systems with continual interchange between Cu^{II} and Cu^I, a major point of interest has been the nature of the change, if any, in the primary co-ordination sphere, concomitant with change in metal oxidation state. Structural characterisation of plastocyanin[1] and azurin,[2] in both their oxidised and reduced forms, has shown that in these biologically occurring molecules reorganisation of the donor set is minimal. In the case of synthetic N$_2$S$_2$ ligands, however, which have been prepared as an aid to understanding the naturally occurring systems, there is a paucity of information pertaining to this; indeed we are only aware of one ligand of this type involving unsaturated N-donors for which crystal structure determinations have been reported on both its copper(I) and copper(II) complexes.[3] The ligand in this case is a quadridentate N$_2$S$_2$ with terminal pyridine-N atoms. In the present study we report on an investigation of the complexing properties of N,N'-bis$\{$[2-(phenylmethylthio)phen-yl]methylene$\}$ethane-1,2-diamine, L, which is a quadridentate N$_2$S$_2$ ligand with terminal thioether donors, during the course of which we have determined the solid-state structure of both its copper(I) and copper(II) complexes as well as the structure of the copper(I) species in nitromethane solution and the electrochemical properties of the system.

Experimental

Proton-decoupled ^{13}C NMR spectra were recorded on a JEOL FX90Q spectrometer. Chemical shifts are quoted on the δ scale

L
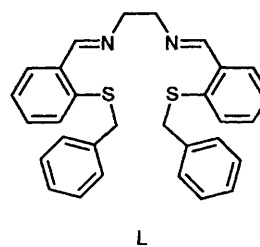
relative to the central peak of the solvent multiplet (CDCl$_3$, 76.95; CD$_3$NO$_2$, 60.55).[4] Sample temperatures are ±1 K and were verified by reference to the ^{1}H NMR spectrum of methanol according to the procedure of van Geet.[5] Molar conductivities were measured with a Philips PW9504 conductivity bridge on 10^{-3} mol dm^{-3} solutions at 293 K. Elemental analyses were performed by the Australian Microanalytical Service. Cyclic voltammetry was conducted in a three-electrode cell having a glassy carbon working electrode, platinum-wire counter electrode and an Ag–AgNO$_3$ reference electrode, on 10^{-3} mol dm^{-3} solutions of complexes in nitromethane with 10^{-1} mol dm^{-3} tetrabutylammonium tetrafluoroborate as supporting electrolyte. The $E_\frac{1}{2}$ values were normalised to the saturated calomel electrode (SCE) via the ferrocene–ferrocenium couple.

Preparation of 2-(phenylmethylthio)benzenemethanol,[6] tetrakis(acetonitrile)copper(I) perchlorate,[7] and barium manganate[8] were carried out according to published procedures.

Preparations.—2-(Phenylmethylthio)benzaldehyde. Barium manganate (30 g, 3 fold excess by mass) was added to a stirred solution of 2-(phenylmethylthio)benzenemethanol (10.0 g, 43.5 mmol) in dichloromethane (200 cm^3). The resulting suspension was stirred at room temperature for 20 h after which the solids were separated by filtration of the reaction mixture through a pad of Kieselguhr. The filtrate and pad washings were dried (MgSO$_4$) and evaporated to dryness. Recrystallisation of the residue twice from ethanol gave the pure product as fine

Table 1 Crystallographic data

	[CuL]ClO$_4$	[CuL(H$_2$O)][ClO$_4$]$_2$
Empirical formula	C$_{30}$H$_{28}$ClCuN$_2$O$_4$S$_2$	C$_{30}$H$_{30}$Cl$_2$CuN$_2$O$_9$S$_2$
M_w	643.4	760.9
Space group	Cc	$P2_1/c$
$a/\text{Å}$	8.277(1)	20.222(1)
$b/\text{Å}$	25.818(1)	7.882(1)
$c/\text{Å}$	13.257(1)	22.708(2)
$\beta/°$	96.24(1)	114.98(1)
$U/\text{Å}^3$	2816(2)	3281(1)
Z	4	4
$F(000)$	1328	1524
$D_c/\text{g cm}^{-3}$	1.518	1.541
$D_m{}^a/\text{g cm}^{-3}$	1.50(1)	1.53(1)
Crystal dimensions/mm	0.13 × 0.22 × 0.37	0.10 × 0.35 × 0.75
μ/cm^{-1}	10.84	10.34
Transmission coefficient	0.83–0.90	0.71–0.92
$\theta_{max}/°$	25	20
hkl	9–9, 0–30, $\overline{15}$–15	$\overline{19}$–19, 0–7, $\overline{22}$–22
T/K	293(2)	293(2)
Scan width/°	0.9 + 0.35 tanθ	1 + 0.35 tanθ
Scan mode	ω–0.7θ	ω–1.3θ
No. of reflections measured	4961	6683
No. used in refinement	4422	1530
R_{int}	—	0.036
No. of parameters refined	359	415
R^b	0.045	0.091
R'	0.057	0.100
Goodness of fit	1.39	2.38
Final shift/error	0.01	0.09

^{a} By flotation in a carbon tetrachloride–hexane mixture. ^{b} $R = \Sigma(|F_o|^2 - |F_c|^2)^2/\Sigma|F_o|^2$.

colourless needles: yield 7.65 g (77%); m.p. 77.5–79.5 °C (lit.,[9] m.p. 75–76 °C) (Found: C, 73.8; H, 5.4. C$_{14}$H$_{12}$OS requires C, 73.7; H, 5.3%). ^{1}H NMR (CDCl$_3$): δ 10.27 (s, 1 H, CH=O), 7.90–7.00 (m, 9 H, aromatic H) and 4.10 (s, 2 H, CH$_2$S).

N,N'-Bis{[2-(phenylmethylthio)phenyl]methylene}ethane-1,2-diamine, L. A solution of 1,2-diaminoethane (0.13 g, 2.2 mmol) in ethanol (10 cm^3) was added to a solution of 2-(phenylmethylthio)benzaldehyde (1.0 g, 4.4 mmol) in ethanol (40 cm^3). After 2 h precipitation of the crude product was complete, whereupon it was collected by filtration and recrystallised once from ethanol giving the pure product as fine colourless prisms: yield 0.91 g (86%), m.p. 127–129 °C (Found: C, 74.9; H, 6.1; N, 6.0. C$_{30}$H$_{28}$N$_2$S$_2$ requires C, 75.0; H, 5.9; N, 5.8%). NMR (CDCl$_3$): ^{1}H, δ 8.77 (s, 2 H, CH=N), 7.98–7.00 (m, 18 H, aromatic H) and 3.93 (s, 8 H, CH$_2$N, CH$_2$S); ^{13}C, δ 160.9 (C=N), 136.9, 136.6, 136.2, 132.3, 130.4, 128.7 (4 C), 128.3 (4 C), 127.7, 127.2, 127.0 (aromatic C), 61.6 (NCH$_2$) and 40.2 (SCH$_2$). IR (Nujol): 1639 cm^{-1} ν (C=N).

N,N'-Bis{[2-(phenylmethylthio)phenyl]methylene}ethane-1,2-diamine-S,S',N,N']copper(I) perchlorate, [CuL]ClO$_4$. A warm solution of L (0.25 g, 0.52 mmol) dissolved in dry deoxygenated ethanol (10 cm^3) was added to a solution of tetrakis(acetonitrile)copper(I) perchlorate (0.17 g, 0.52 mmol) in ethanol (10 cm^3), which had been prepared under dry argon. The resulting solution was allowed to stand for 1 h after which orange crystals of the pure product were collected by filtration in an inert atmosphere, washed with deoxygenated ethanol (2 × 5 cm^3) and dried under vacuum. Yield: 0.30 g (90%); m.p. 168.5–170.0 °C. The pure product is air stable indefinitely, when in the solid state (Found: C, 56.3; H, 4.2; N, 4.4. C$_{30}$H$_{28}$ClCuN$_2$O$_4$S$_2$ requires C, 56.0; H, 4.4; N, 4.4%). ^{13}C NMR (CD$_3$NO$_2$, 370 K): δ 162.6 (C=N), 136.2, 134.6, 133.8, 131.4, 129.5, 128.3 (4 C), 127.7 (4 C), 127.4, 127.2 (4 C, aromatic C), 61.7 (NCH$_2$) and 44.2 (SCH$_2$). Λ$_M$ (MeNO$_2$): 75 Ω^{-1} cm^2 mol^{-1} (1:1).[10] Electronic spectrum λ$_{max}$/nm(EtOH): 222 (ε/dm^3 mol^{-1} cm^{-1} 33 000), 294 (6600), 341 (2300) and 407 (990).

Aqua(N,N'-bis{[2-(phenylmethylthio)phenyl]methylene}-

ethane-1,2-diamine-S,S',N,N')copper(II) perchlorate, [CuL-(H$_2$O)][ClO$_4$]$_2$. Hexaaquacopper(II) perchlorate (0.37 g, 1 mmol) dissolved in ethanol (10 cm^3) was added to a solution of L (0.24 g, 0.5 mmol) in ethanol (10 cm^3). The mixture was heated under reflux for 5 min and allowed to cool. The greenish brown precipitate was collected by filtration, washed with cold ethanol (2 × 15 cm^3) and dried overnight under vacuum. Yield: 0.34 g (93%); m.p. 145–147 °C (Found: C, 47.0; H, 3.8; N, 3.7. C$_{30}$H$_{30}$Cl$_2$CuN$_2$O$_9$S$_2$ requires C, 47.3; H, 3.9; N, 3.7%). Λ$_M$ (MeNO$_2$): 170 Ω^{-1} cm^2 mol^{-1} (1:2).[10] Magnetic moment: μ$_{eff}$ = 1.92 μ$_B$. Visible spectrum λ$_{max}$/nm(MeNO$_2$) 550 (ε/dm^3 mol^{-1} cm^{-1} 470).

Structural Analyses.—Single crystals of [CuL]ClO$_4$ were grown from an ethanolic solution which had been prepared and maintained under anaerobic and anhydrous conditions. Exposure of the mother-liquor to the atmosphere led to slow deposition of further material in the form of single crystals of [CuL(H$_2$O)][ClO$_4$]$_2$. Unit-cell and intensity data were measured with a CAD-4 diffractometer using graphite-monochromated Mo-Kα X-radiation. Unit-cell parameters (Table 1) were determined from a least-squares fit to the setting angles of 25 reflections chosen widely in reciprocal space each at four different values of ψ in the θ range 13–20° for the copper(I) complex and 10–17° for the copper(II) complex, λ = 0.710 69 Å. Space groups were determined from precession photographs, with *Cc* ultimately chosen for the copper(I) complex on the basis of the structure solution and refinement. Three reflections monitored every 120 min showed no significant variation in intensity. Absorption corrections were applied (Gaussian quadrature, 10 × 10 × 10 grid). Crystals of the copper(II) complex were of very poor quality and diffracted weakly, 3071 of the 6683 reflections sampled had σ(*I*)/*I* < 2 on the fast scan and were not remeasured.

Both crystal structures were solved by Patterson and Fourier methods. Although hydrogen atom positions could be seen in difference maps for the copper(I) complex they were placed in calculated positions for both structures with arbitrarily assigned

Table 2 Atomic positional parameters with estimated standard deviations (e.s.d.s) in parentheses

(a) [CuL]+ *

Atom	X/a	Y/b	Z/c
Cu	0	-0.148 07(2)	-1/4
S(1)	0.091 7(1)	-0.227 89(3)	-0.195 67(8)
N(1)	0.135 0(4)	-0.113 2(1)	-0.132 2(2)
C(1)	0.047 4(6)	-0.068 1(2)	-0.099 6(3)
C(2)	0.261 0(5)	-0.129 2(2)	-0.077 4(3)
C(3)	0.359 7(4)	-0.174 4(1)	-0.099 5(3)
C(4)	0.303 9(4)	-0.218 4(1)	-0.156 4(3)
C(5)	0.415 0(5)	-0.257 1(2)	-0.172 9(3)
C(6)	0.578 0(5)	-0.252 9(2)	-0.135 2(4)
C(7)	0.631 0(5)	-0.210 6(2)	-0.078 1(3)
C(8)	0.523 2(5)	-0.172 9(2)	-0.059 2(3)
C(9)	0.086 3(5)	-0.278 6(2)	-0.292 9(3)
C(10)	-0.086 2(5)	-0.297 7(1)	-0.315 0(3)
C(11)	-0.200 9(5)	-0.270 1(1)	-0.375 1(3)
C(12)	-0.359 9(5)	-0.289 1(2)	-0.394 7(3)
C(13)	-0.401 4(5)	-0.335 9(2)	-0.356 3(3)
C(14)	-0.286 2(6)	-0.364 6(2)	-0.297 3(4)
C(15)	-0.129 4(5)	-0.345 2(2)	-0.277 0(3)
S(1')	-0.083 9(1)	-0.129 35(3)	-0.413 73(7)
N(1')	-0.187 5(4)	-0.108 4(1)	-0.193 1(2)
C(1')	-0.131 3(5)	-0.082 0(2)	-0.097 9(3)
C(2')	-0.322 9(5)	-0.096 9(2)	-0.240 7(3)
C(3')	-0.390 1(4)	-0.122 3(1)	-0.335 8(3)
C(4')	-0.300 6(4)	-0.137 8(1)	-0.414 5(3)
C(5')	-0.377 5(4)	-0.160 8(2)	-0.501 5(3)
C(6')	-0.542 6(5)	-0.171 8(2)	-0.508 4(3)
C(7')	-0.630 6(5)	-0.157 8(2)	-0.430 9(3)
C(8')	-0.558 4(5)	-0.132 3(2)	-0.346 7(3)
C(9')	-0.074 3(5)	-0.059 9(2)	-0.443 8(3)
C(10')	0.100 1(4)	-0.044 8(1)	-0.455 0(3)
C(11')	0.191 0(5)	-0.018 3(2)	-0.380 2(3)
C(12')	0.347 8(5)	-0.002 3(2)	-0.394 1(4)
C(13')	0.412 6(5)	-0.013 7(2)	-0.482 0(4)
C(14')	0.323 4(6)	-0.041 3(2)	-0.556 4(4)
C(15')	0.166 7(5)	-0.057 2(2)	-0.544 9(3)

(b) [CuL(H2O)]2+

Atom	X/a	Y/b	Z/c
Cu	0.319 4(1)	0.158 5(3)	0.069 8(1)
O(5)	0.286 1(6)	0.438(1)	0.058 1(6)
S(1)	0.398 9(2)	0.169 6(7)	0.020 2(2)
N(1)	0.396 2(8)	0.182(2)	0.157 0(7)
C(1)	0.366(1)	0.177(3)	0.204 4(9)
C(2)	0.462(1)	0.197(3)	0.182(1)
C(3)	0.509 8(9)	0.206(2)	0.147(1)
C(4)	0.488 3(9)	0.199(2)	0.082(1)
C(5)	0.543(1)	0.205(2)	0.057(1)
C(6)	0.616(1)	0.224(3)	0.098(1)
C(7)	0.641(1)	0.234(3)	0.163(1)
C(8)	0.586(1)	0.219(2)	0.186 5(9)
C(9)	0.384(1)	0.363(2)	-0.027(1)
C(10)	0.320 4(9)	0.339(3)	-0.093 2(9)
C(11)	0.323(1)	0.228(3)	-0.139(1)
C(12)	0.263(2)	0.205(3)	-0.198(1)
C(13)	0.197(1)	0.303(4)	-0.207(1)
C(14)	0.198(2)	0.415(3)	-0.163(1)
C(15)	0.256(1)	0.437(3)	-0.104(1)
S(1')	0.2261(3)	0.089 8(6)	-0.030 0(2)
N(1')	0.256 4(8)	0.088(2)	0.114 0(7)
C(1')	0.306(1)	0.043(2)	0.181 7(9)
C(2')	0.189(1)	0.097(2)	0.097(1)
C(3')	0.134 7(9)	0.143(2)	0.031(1)
C(4')	0.145(1)	0.153(2)	-0.026(1)
C(5')	0.088(1)	0.204(3)	-0.082(1)
C(6')	0.021(1)	0.252(3)	-0.085(1)
C(7')	0.012(1)	0.243(3)	-0.030(1)
C(8')	0.068(1)	0.191(3)	0.031(1)
C(9')	0.215 9(9)	-0.141(3)	-0.032 3(9)
C(10')	0.152(1)	-0.190(2)	-0.093 1(9)
C(11')	0.149(1)	-0.155(3)	-0.154(1)
C(12')	0.089(2)	-0.194(3)	-0.212(1)
C(13')	0.030(1)	-0.273(3)	-0.208(1)
C(14')	0.032(1)	-0.313(3)	-0.148(1)
C(15')	0.093(1)	-0.275(3)	-0.093(1)

* Coordinates of the perchlorate groups for both structures are available as supplementary data.

isotropic thermal parameters. The water-molecule hydrogen atoms were not included. Non-hydrogen atomic coordinates and anisotropic thermal parameters were refined by full-matrix least squares minimising $\Sigma w(|F_o|^2 - |F_c|^2)^2$ where $w = 1/\sigma^2$-(F_o^2) and $\sigma(F_o^2)$ was obtained from counting statistics for the copper(I) complex and a combination of counting statistics and mean deviations for the copper(II) complex. Hydrogen atom coordinates and thermal parameters were not refined.

Computer programs of the XTAL system [11] were used in the structure determination and refinement; CRYLSQ [12] was used for least-squares refinement with neutral atom scattering factors for all atoms. A refinement summary appears in Table 1.

The perchlorate anion associated with Cl(1) of the copper(II) complex is severly disordered. Several attempts to model the disorder by introducing rigid groups with partial occupancy failed significantly to improve the model. Finally, the group was refined with individual anisotropic thermal parameters for all the atoms. This course gave rise to very large 'thermal' ellipsoids, and although accounting for much of the electron density in the region there were many peaks in the range −0.44 to +0.59 e Å⁻³ remaining in the final difference map. Several of the ligand 'thermal' ellipsoids are also clearly not due to thermal motion of the atoms, but rather represent the best fit of the model to the poor data obtainable from these crystals. Maximum and minimum residual electron density in the final difference map for the copper(I) complex were +0.54 and −0.41 e Å⁻³, again near the perchlorate group.

The final positional coordinates are given in Table 2. The

Flack absolute structure parameter [13] refined to −0.01(1) for the listed coordinates indicating that they correspond to the correct chirality-polarity for the crystal used in the data collection.

Additional material available from the Cambridge Crystallographic Data centre comprises H-atom coordinates, thermal parameters and remaining bond lengths and angles.

Results and Discussion

Syntheses.—Ligand L was prepared in high yield by Schiff-base condensation of 1,2-diaminoethane with 2-(phenylmethyl-thio)benzaldehyde. Addition of L, under anaerobic and anhydrous conditions, to a solution of [Cu(MeCN)₄]ClO₄ turned the solution bright orange and led to the precipitation of air-stable crystals of [CuL]ClO₄. Exposure of the supernatant solution to air, however, led to oxidation of the metal, accompanied by the uptake of water, and gradual deposition of brown crystals of [CuL(H₂O)][ClO₄]₂. Direct reaction of hydrated copper(II) perchlorate with L in ethanol also produces [CuL(H₂O)][ClO₄]₂.

Crystal and Molecular Structure of [CuL]ClO₄.—The asymmetric copper(I) ion in [CuL]ClO₄ has a highly distorted tetrahedral geometry (Fig. 1 and Table 3). The CuN₂–CuS₂ dihedral angle is 60.0(1)°. The distortion probably arises from the combined effects of the relatively small bite of the 1,2-diaminoethane chelating moiety, which pinches two tetrahedral vertices together, causing a consequential opening of the
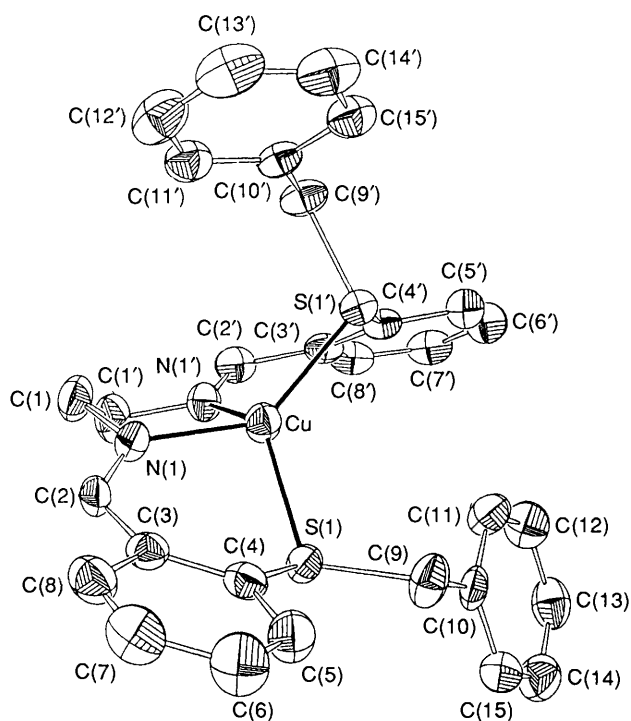
Fig. 1   A perspective drawing of the [CuL]⁺ cation showing thermal ellipsoids of the non-hydrogen atoms at the 50% probability level
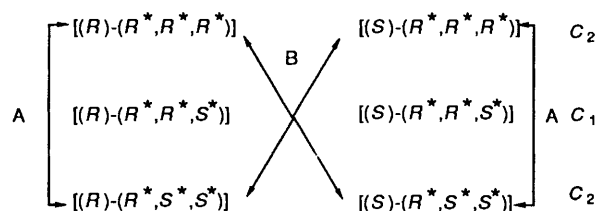

Fig. 2   The stereochemistry and symmetry associated with the three different diastereomers of [CuL]⁺ and their enantiomers.† Pathway A indicates interconversion between the two diastereomers observed in CD₃NO₂ solution accomplished by inversion of both sulfur atoms. Pathway B indicates the related interconversion achieved by changing the helicity of the ligand to metal attachment

Table 3   Selected bond lengths (Å) and angles (°)

	[CuL]ClO₄	[CuL(H₂O)][ClO₄]₂
Cu–S(1)	2.285(1)	2.323(6)
Cu–S(1′)	2.258(1)	2.318(5)
Cu–N(1)	2.029(3)	1.94(1)
Cu–N(1′)	2.069(3)	2.00(2)
Cu–O(5)	—	2.29(1)
C(1)–C(1′)	1.524(6)	1.53(3)
C(1)–N(1)	1.464(5)	1.44(3)
N(1)–C(2)	1.274(5)	1.22(2)
C(2)–C(3)	1.472(5)	1.48(4)
C(3)–C(4)	1.412(5)	1.35(3)
C(4)–S(1)	1.794(4)	1.78(2)
S(1)–C(9)	1.834(4)	1.81(2)
S(1)–Cu–S(1′)	123.56(4)	88.8(2)
S(1)–Cu–N(1)	91.20(9)	94.1(6)
S(1)–Cu–N(1′)	124.62(9)	165.9(5)
S(1′)–Cu–N(1)	136.97(9)	171.6(5)
S(1′)–Cu–N(1′)	94.59(9)	89.9(4)
N(1)–Cu–N(1′)	82.7(1)	85.4(7)
O(5)–Cu–N(1)	—	95.5(6)
O(5)–Cu–N(1′)	—	96.2(6)
O(5)–Cu–S(1)	—	97.9(4)
O(5)–Cu–S(1′)	—	91.9(3)

opposing two, and the steric constraints imposed by the tendency to maintain extended conjugation within the six-membered chelate rings. This tendency is not fully realised, however, as the dihedral angles between the aromatic rings and the adjacent imino moiety are significant: −27.4(6) and −38.3(6)° for N(1)–C(2)–C(3)–C(4) and N(1′)–C(2′)–C(3′)–C(4′) respectively. The Cu–S bond distances show the slight shortening which usually accompanies expansion of a S–Cu–S angle towards 180°[14,15] while Cu–N distances are typical for copper(I)–imino nitrogen contacts.[15,16] The dihedral angle N(1)–C(1)–C(1′)–N(1′) within the ethylene linkage is −47.3(4)°.

The cation [CuL]⁺ is inherently dissymmetric, owing to the helical attachment of L to the metal, which gives rise to R- and S-enantiomeric forms of the complex. In addition the overall stereochemistry is determined by the chirality at each of the two sulfur stereocentres, which can be either R or S when co-ordinated. Thus there are three possible diastereomers of [CuL]⁺, each of which has a non-superimposable mirror image form, as shown in Fig. 2. It can be seen from Fig. 1 that the molecular asymmetry originates from the fact that in the solid state the two sulfur atoms have opposing chirality. The unit cell is comprised of equal numbers of right handed, $[R$-$(R^*,R^*,S^*)]$,† and left handed, $[S$-$(R^*,R^*,S^*)]$, cations, which are related by a glide plane.

Solution Structure of [CuL]⁺.—Dissolution of [CuL]ClO₄ in dry, deoxygenated CD₃NO₂ and observation of its ¹³C-{¹H} NMR spectrum at elevated temperatures reveals singlet resonances for the imino, benzylic, and methylene carbon atoms (the last resonance is obscured beneath a solvent peak at some temperatures) as well as a multiplet of resonances arising from the aromatic carbons. This spectrum is indicative of a diastereomer having C_2 symmetry and not the C_1 diastereomer observed in the solid state. Lowering the sample temperature leads to a splitting of these resonances into asymmetric doublets, which is particularly evident for the imino and benzylic signals (δ 162.6 and 44.2, respectively), as may be seen in Fig. 3. The asymmetrical intensity of the split signals is also inconsistent with the presence of the $[(\pm)$-$(R^*,R^*,S^*)]$ diastereomer, as this would show symmetrical pairs of resonances arising from each type of carbon atom, but rather points to an interconversion between the C_2 diastereomers, which is fast on the NMR timescale at elevated temperatures, and which could proceed by either pathway A or B shown in Fig. 2. Application of the Eyring equation[17] gives $\Delta G^{\ddagger}_{280} = 59.8 \pm 0.6$ kJ mol⁻¹ for this process.

The major and minor resonances appear in the intensity ratio 2.6 : 1 at 252 K corresponding to an equilibrium constant for the major ⟶ minor diastereomer conversion of 0.38 and $\Delta G° = 2$ kJ mol⁻¹. The identity of each diastereomer can be established from the relative chemical shifts of the two benzylic resonances in the following way. Reference to Fig. 1, which shows the $[(R)$-$(R^*,R^*,S^*)]$ form of the complex with S(1′)R and S(1)S, indicates that a benzylic carbon atom attached to an R^*,R^* sulfur atom, C(9′), is held above the plane of the chelating aromatic ring whilst a benzylic carbon atom attached to an R^*,S^* sulfur atom, C(9), is much closer to coplanarity with the chelating aromatic ring. It follows, therefore, that the major diastereomer, with the downfield benzylic resonance, is most likely the $[(\pm)$-$(R^*,S^*,S^*)]$ and the minor the $[(\pm)$-$(R^*,R^*,R^*)]$. If any $[(\pm)$-$(R^*,R^*,S^*)]$ is present in CD₃NO₂

---

† Stereochemical descriptors used here are consistent with recent Chemical Abstracts indexing practice: within the group of relative configurations (asterisked) the first refers to the chirality at the metal ion followed by that at the two (otherwise equivalent) sulfur atoms. The absolute configuration descriptor refers to the chirality at the metal ion.
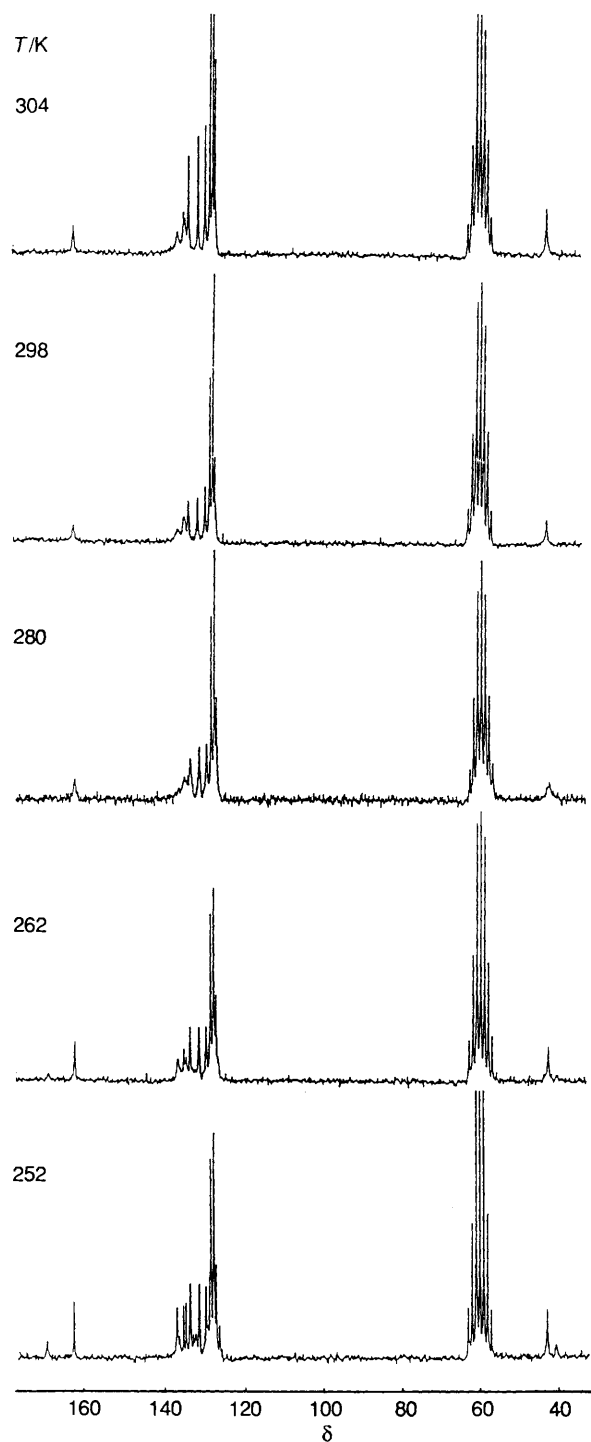
T/K

304

298

280

262

252

160   140   120   100   80   60   40
δ

Fig. 3 Variable-temperature ^{13}C-{^{1}H} NMR spectra of [CuL]ClO$_4$ in CD$_3$NO$_2$ showing the equilibrium between [($\pm$)-(R^*,R^*,R^*)] and [($\pm$)-(R^*,S^*,S^*)] diastereomers

Fig. 4 Energy profile for the diastereomers of [CuL]Clo$_4$. The value of $\Delta G^{\ddagger}$ applies at 280 K, values of ΔG° apply at 252 K

Fig. 5 A perspective drawing of the [CuL(H$_2$O)]$^{2+}$ cation showing thermal ellipsoids of the non-hydrogen atoms at the 50% probability level

solution it must be at a concentration below the limits of detectability by NMR spectroscopy. This implies that K for the [($\pm$)-(R^*,S^*,S^*)] to [($\pm$)-(R^*,R^*,S^*)] interconversion is $< \approx 0.1$ ($\Delta G^{\circ} > \approx 6$ kJ mol^{-1}). On the basis of these data the energy profile for this group of diastereomers is shown in Fig. 4. It is interesting that the crystallisation-induced disequilibration favours the least stable diastereomer; although this is not without precedent for this type of ligand.[18]

Fig. 2 indicates that the interconversions observed in the ^{13}C NMR spectra may proceed by two different routes. The data available to us do not indicate which, or whether both are operative. Pathway A involves inversion at both sulfur atoms,
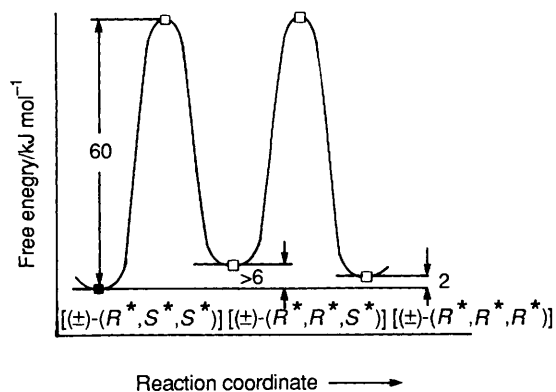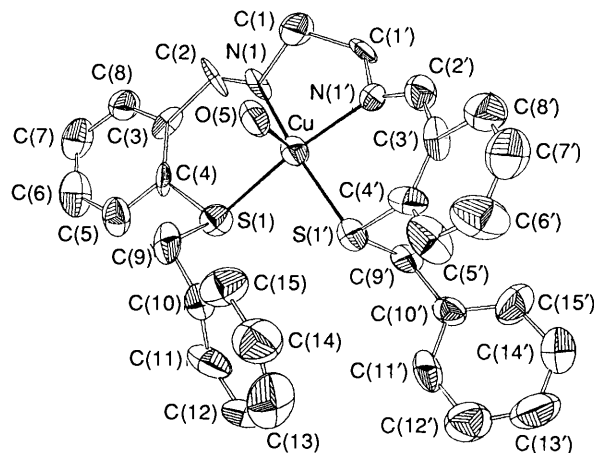
following the reaction coordinate of Fig. 4, without a change in helicity at the metal stereocentre. For inversion of co-ordinated thioethers $\Delta G^{\ddagger}$ is typically around 60 kJ mol^{-1},[19] agreeing closely with the value measured here, and making this a possible mechanism. Pathway B, however, which involves only a change of helicity at the metal, can be followed by three different means:[20] (i) bond rupture of two or more metal–ligand bonds followed by reformation of each in the opposite sense; (ii) inversion of the tetrahedral metal centre via a square-planar intermediate; (iii) intermolecular ligand exchange. There are no quantitative data available, concerning any of these sub-pathways, which can be meaningfully related to [CuL]$^+$ and compared with the measured value of $\Delta G^{\ddagger}$. It is well known, though, that copper(I)–thioether bonds are labile[21] and on these grounds alone it would be surprising if sub-pathway (i) were not a contributor. We have investigated sub-pathway (iii), by adding additional ligand to the NMR sample of [CuL]$^+$, and observe formation of [CuL$_2$]$^+$ as a stable entity suggesting that this sub-pathway could also be used to effect the interconversion. The structure and properties of [CuL$_2$]$^+$ are currently under investigation and will be reported in due course.

Crystal and Molecular Structure of [CuL(H$_2$O)][ClO$_4$]$_2$.—Oxidation of [CuL]ClO$_4$ under aerobic conditions is accompanied by aquation of the metal centre and the formation of the square-pyramidal complex [CuL(H$_2$O)][ClO$_4$]$_2$ which has the water molecule at the apical position of the Cu^{II} ion (Fig. 5). The four donor atoms of the quadridentate ligand are coplanar and the metal ion lies 0.2 Å above this plane in the direction of the water molecule. Both sulfur atoms have the same chirality leading to Cu–S bond distances which are the same within experimental error (2.321 Å, average), and slightly longer than
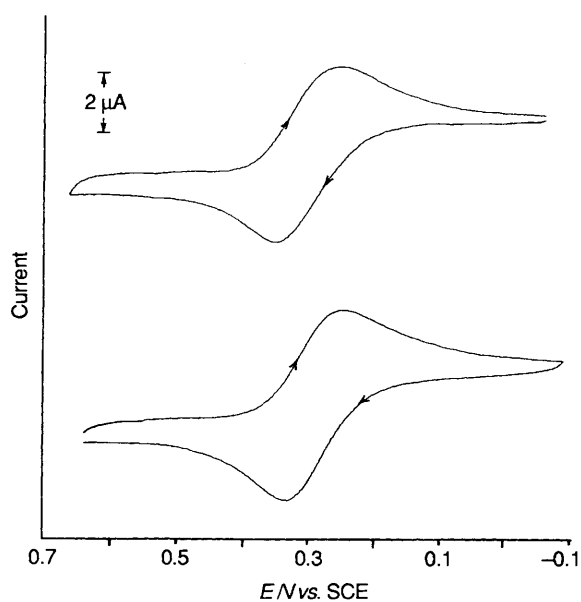
Fig. 6 Cyclic voltammograms for [CuL]ClO$_4$, upper trace, and [CuL-(H$_2$O)][ClO$_4$]$_2$, lower trace

in [CuL]$^+$ (Table 3). Previously, bond lengths to Cu^{II} have been found to be shorter than corresponding bond lengths to Cu^{I},[1-3] owing to the smaller covalent radius of Cu^{II}. The reversal observed here arises from the shorter than average Cu^{I}–S bond length, associated with the large S–Cu–S angle, which we commented on above. The Cu–N bond lengths in [CuL(H$_2$O)]$^{2+}$ are shorter than those for [CuL]$^+$. Because of the R^*,R^* configuration of the ligand the molecule is asymmetric and the unit cell is comprised of both enantiomeric forms. Both perchlorate ions are hydrogen-bonded to the water molecule with closest contacts of 2.82(2) [O(5)···O(2)] and 2.95(2) [O(5)···O(1')] Å. The oxygen atom of one perchlorate ion [O(3)] is directed towards the vacant apical site of the Cu^{II} ion and is at a distance of 3.12(1) Å from it.

Electrochemistry.—The redox behaviour of the complexes was investigated by cyclic voltammetry in nitromethane solution. The results obtained are consistent with a quasi-reversible one-electron transfer and are shown in Fig. 6. The two complexes show slightly different $E_{\frac{1}{2}}$ values, 0.29 and 0.27 V *vs.* SCE for the Cu^{I} and Cu^{II} species, which may arise from the fact that water is absent from the system when [CuL]ClO$_4$ is used to initiate the cycle. The anodic-to-cathodic peak potential separations are 0.098 and 0.089 V, at a scan rate of 10 mV s^{-1}, for the copper(I) and copper(II) species respectively. The ratio of anodic-to-cathodic peak currents is very close to unity in both

cases. The $E_{\frac{1}{2}}$ values observed here match closely those found for a pair of related macrocyclic copper(II)N$_2$S$_2$ complexes, but differ markedly from that found for the copper(II) complex of the methylthio analogue of L for which $E_{\frac{1}{2}}$ = 0.42 V *vs.* SCE in MeCN.[22,23] It appears, therefore, that the inflexibility of the macrocyclic ligands is paralleled by the bulkiness of the benzyl groups and that none of the ligands can accommodate the regular tetrahedral geometry preferred by Cu^{I} as readily as the methylthio analogue of L.

References

1 J. M. Guss, P. R. Harrowell, M. Murata, V. A. Noris and H. C. Freeman, *J. Mol. Biol.*, 1986, **192**, 361.
2 W. E. B. Shepard, B. F. Anderson, D. A. Lewandoski, G. E. Norris and E. N. Baker, *J. Am. Chem. Soc.*, 1990, **112**, 7817.
3 G. R. Brubaker, J. N. Brown, M. K. Yoo, R. A. Kinsey, T. M. Kutchan and E. A. Mottel, *Inorg. Chem.*, 1979, **18**, 299.
4 E. Breitmaier, G. Haas and W. Voelter, *Atlas of Carbon-13 NMR Data*, Heyden, London, 1979, vol. 1.
5 A. E. van Geet, *Anal. Chem.*, 1970, **42**, 679.
6 G. W. Stacey, F. W. Villaescusa and T. E. Wollner, *J. Org. Chem.*, 1965, **30**, 4074.
7 P. Hemmerich and C. Sigwart, *Experientia*, 1963, **19**, 488; G. J. Kubas, *Inorg. Synth.*, 1976, **19**, 90.
8 H. Firouzabadi and Z. Mostafavipoor, *Bull. Chem. Soc. Jpn.*, 1983, **56**, 914.
9 G. W. Stacey, D. L. Eck and T. E. Wollner, *J. Org. Chem.*, 1970, **35**, 3495.
10 W. J. Geary, *Coord. Chem. Rev.*, 1971, **7**, 81.
11 S. R. Hall and J. M. Stewart (Editors), XTAL 3.0 Reference Manual, Universities of Western Australia and Maryland, 1990.
12 R. Olthof-Hazekamp, CRYSLQ, XTAL 3.0 Reference Manual, eds. S. R. Hall and J. M. Stewart, Universities of Western Australia and Maryland, 1990.
13 H. D. Flack, in *Crystallographic Computing 4: Techniques and New Technologies*, eds. N. W. Isaacs and M. R. Taylor, Oxford University Press, 1988, pp. 143–144.
14 P. R. W. Corfield, C. Ceccarelli, M. D. Glick, W. Y. Moy, L. A. Orchrymowycz and D. B. Rorabacher, *J. Am. Chem. Soc.*, 1985, **107**, 2399.
15 J. W. L. Martin, G. J. Organ, K. P. Wainwright, K. D. V. Weerasuria, A. C. Willis and S. B. Wild, *Inorg. Chem.*, 1987, **26**, 2963.
16 P. C. Healy, L. M. Engelhardt, V. A. Patrick and A. H. White, *J. Chem. Soc., Dalton Trans.*, 1985, 2541.
17 H. Shanan-Atidi and K. H. Bar-Eli, *J. Phys. Chem.*, 1970, **74**, 961.
18 J. M. Csavas, M. R. Taylor and K. P. Wainwright, *J. Chem. Soc., Dalton Trans.*, 1988, 2573.
19 E. W. Abel, S. K. Bhargava and K. G. Orrell, *Prog. Inorg. Chem.*, 1984, **32**, 1.
20 S. S. Eaton and R. H. Holm, *Inorg. Chem.*, 1971, **10**, 1446.
21 S. G. Murray and F. R. Hartley, *Chem. Rev.*, 1981, **81**, 365.
22 A. W. Addison, T. N. Rao and E. Sinn, *Inorg. Chem.*, 1984, **23**, 1957.
23 P. Zanello, *Comments Inorg. Chem.*, 1988, **8**, 45.